Errors–in–variables identification using maximum likelihood estimation in the frequency domain

September 9, 2016

Torsten Söderström[1] and Umberto Soverini[2]
[1]Department of Information Technology, Uppsala University, Sweden
[2]Department of Electrical, Electronic and Information Engineering, University of Bologna, Italy

Abstract

This report deals with the identification of errors–in–variables (EIV) models corrupted by additive and uncorrelated white Gaussian noises when the noise–free input is an arbitrary signal, not required to be periodic. In particular, a frequency domain maximum likelihood (ML) estimator is proposed and analyzed in some detail. As some other EIV estimators, this method assumes that the ratio of the noise variances is known. The estimation problem is formulated in the frequency domain. It is shown that the parameter estimates are consistent. An explicit algorithm for computing the asymptotic covariance matrix of the parameter estimates is derived. The possibility to effectively use lowpass filtered data by using only part of the frequency domain is discussed, analyzed and illustrated.

1 Introduction

In this report the problem of identifying a linear dynamic system from noisy input–output measurements is addressed. System representations where both inputs and outputs are affected by additive errors are called errors–in–variables (EIV) models and play an important role in several engineering and other applications, Van Huffel (1997), Van Huffel and Lemmerling (2002), Zhang *et al.* (2013). Many system identification methods have been proposed for the EIV problems. For some surveys in the field, see Söderström (2007), Söderström (2012) and Guidorzi *et al.* (2008).

In many EIV contexts the additive noises are assumed as white. In these cases, if the assumptions of Gaussianity are fulfilled, it is feasible to use a maximum likelihood (ML) approach. In this work the EIV ML problem is addressed by using frequency domain techniques, when the noise-free input is an arbitrary sequence and the noise variance ratio is known. The frequency domain approach has some special features, not present in time domain methods. In particular, filtering can be reduced to the selection of appropriate frequencies in a limited band of the signal spectrum. Moreover, continuous-time and discrete-time models can be handled with equal difficulties, McKelvey (2002), Ljung (1999). From a theoretic point of view, there is a full equivalence between time and frequency domain identification methods, also for finite data records, Agüero *et al.* (2010). Some ideas of the approach described here were first presented in Soverini and Söderström (2014). The derivation here is quite different and much more direct. Further, this report also contains analysis of the consistency and accuracy properties of the parameter estimates. In its approach the report differs from other previous work on an ML formulation of the EIV problem in the time and frequency domains, cf. Diversi *et al.* (2007), Pintelon and Schoukens (2007), Pintelon and Schoukens (2012), see also Zhang *et al.* (2013). The relation of these papers to the present one is discussed in Section (2), see Remark 2.1 and the discussion thereafter.

The organization of the report is as follows. Section 2 defines the EIV identification problem in frequency domain. Section 3 describes the EIV set up in the frequency domain, while Section 4 presents the ML solution. Section 5 analyses the properties of the parameter estimates. In Section 6 the properties of the proposed ML algorithm are verified by means of Monte Carlo simulations. Finally some concluding remarks are reported in Section 7.

2 Statement of the problem

Consider the linear time–invariant SISO system described in Figure 1. The noise–free input and output $u_0(t)$, $y_0(t)$ are linked by the difference equation

$$A(q^{-1})\, y_0(t) = B(q^{-1})\, u_0(t), \tag{1}$$

where $A(q^{-1})$ and $B(q^{-1})$ are polynomials in the backward shift operator q^{-1}

$$\begin{array}{rcl} A(q^{-1}) & = & 1 + a_1\, q^{-1} + \cdots + a_{n_a}\, q^{-n_a} \\ B(q^{-1}) & = & b_0 + b_1\, q^{-1} + \cdots + b_{n_b}\, q^{-n_b}. \end{array} \tag{2}$$

In the EIV environment the input and output measurements are assumed to be cor-

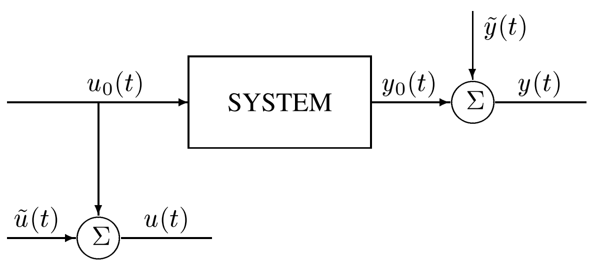

Figure 1: The basic setup for a dynamic errors-in-variables problem.

rupted by additive noise so that the available observations are

$$u(t) = u_0(t) + \tilde{u}(t) \quad (3)$$

$$y(t) = y_0(t) + \tilde{y}(t). \quad (4)$$

In the sequel, the following assumptions will be considered as satisfied.

A1. The system (1) is asymptotically stable.

A2. $A(q^{-1})$ and $B(q^{-1})$ do not share any common factor.

A3. The polynomial degrees n_a and n_b are assumed to be *a priori* known.

A4. The noiseless input $u_0(t)$ is a zero–mean ergodic process and is persistently exciting of sufficiently high order.

A5. $\tilde{u}(t)$ and $\tilde{y}(t)$ are mutually uncorrelated zero–mean Gaussian white processes with variances λ_u and λ_y, respectively.

A6. $\tilde{u}(t)$ and $\tilde{y}(t)$ are uncorrelated with the noise–free input $u_0(t)$.

Let $\{u(t)\}_{t=0}^{N-1}$ and $\{y(t)\}_{t=0}^{N-1}$ be a set of input and output observations at N equidistant time instants. The corresponding Discrete Fourier Transforms (DFTs) are defined as

$$U(\omega_k) = \frac{1}{\sqrt{N}} \sum_{t=0}^{N-1} u(t)\, \mathrm{e}^{-j\omega_k t} \;, \quad (5)$$

$$Y(\omega_k) = \frac{1}{\sqrt{N}} \sum_{t=0}^{N-1} y(t)\, \mathrm{e}^{-j\omega_k t} \;, \quad (6)$$

where $\omega_k = 2\pi k/N$ and $k = 0, \ldots, N-1$. In frequency domain, the problem under investigation can be stated as follows.

Problem 1. Let $U(\omega_k)$, $Y(\omega_k)$ be a set of noisy measurements generated by an EIV system of type (1)–(4), under Assumptions A1–A6, where $\omega_k = 2\pi k/N$ and $k = 0, \ldots, N-1$. Estimate the system parameters a_i $(i = 1, \ldots, n_a)$, b_i $(i = 0, \ldots, n_b)$ and possibly the noise variances λ_u, λ_y.

Remark 2.1 *Under the previous Assumptions A1–A6, the system is not identifiable in the very general case. To achieve identifiability, one has to add one of the following assumptions.*

1. *The properties of the noise-free input is given by a model of finite order, for example an ARMA model.*

2. *The noise-free input is known to be periodic. Two periods of the data are then sufficient.*

3. *The ratio of the noise variances is known.*

One can always debate which assumption is more realistic or more general than the others.

The first assumption is applied in the so called joint output method, Söderström (1981). A frequency domain variant is developed in Pintelon and Schoukens (2007).

A reason why the last two assumptions are quite similar in character goes as follows: if the second assumptions applies, by subtracting data of one period from the other period, one gets an estimate of the pure noisy data, and then the noise variances can be estimated separately. This is essentially the SML approach proposed in Schoukens et al. *(1997).*

There are also several methods in the literature where none of the conditions (1) - (3) is imposed, but then the information in the data is not fully exploited. Still, consistency is achieved. Examples of such methods are the instrumental variable method, the generalized instrumental variable method, Söderström (2011), including its special cases bias-eliminating least squares and the Frisch scheme, and the covariance matching approach, Söderström *et al.* (2009).

Methods for EIV identification do also differ in what quantities are estimated in addition to the polynomial coefficients in (2). Both in Zhang *et al.* (2013) and in this report the realization $u_0(0), \ldots, u_0(N-1)$ of the noiseless input is regarded as a deterministic sequence to be estimated.

In this report the following additional assumption is applied, with the aim of deriving, exploiting and analyzing the frequency domain ML estimator.

A7. The noise variances λ_u and λ_y are unknown but their ratio $\rho = \lambda_y/\lambda_u$ is assumed as known, with $0 < \rho < \infty$.

For situations where $\tilde{u}(t)$ and $\tilde{y}(t)$ are due to sensor noise, it can be possible to obtain separate measurement data of the noise only. From such records, estimates of λ_u and λ_y (and also ρ) can be obtained.

Remark 2.2 *It is worth noting that Assumption A7 is necessary also for estimators based on total least squares (TLS), to be consistent, cf. Cadzow and Solomon (1986), Van Huffel (1997), Van Huffel and Lemmerling (2002).*

The paper Zhang *et al.* (2013) uses frequency domain properties as in this report, and both papers take effects of transients into account. While this report deals fully with the ML estimation, the estimation method considered in Zhang *et al.* (2013) is different and only partly based on equations derived from the gradient of the likelihood function.

The following frequency domain property is worth recalling.

Property. Let $x(t)$ be an arbitrary signal. Consider the frequency domain data $X(\omega_k), k = 0, \ldots, N-1$ of of $x(t)$, see (5). The number of data N is usually even, however the following consideration holds also when N is odd. It can be observed that

$$X(\omega_{N-1-k}) = \frac{1}{\sqrt{N}} \sum_{t=0}^{N-1} x(t)\, e^{-j \frac{N-1-k}{N} 2\pi t}$$
$$= \frac{1}{\sqrt{N}} \sum_{t=0}^{N-1} x(t)\, e^{-j \frac{-(1+k)}{N} 2\pi t} = X^*(\omega_{1+k}) \;, \tag{7}$$

where $X^*(\cdot)$ is the conjugate of $X(\cdot)$. The conclusion is that it is enough to consider half of the sequence $X_0, \ldots, X_{N-1}$, since the whole sequence contains redundant information. As a general rule, the identification procedure that will be described in Section 4 can be set up by using only the first

$$M = \text{floor}\,\big(N/2\big) \tag{8}$$

input–output samples U_k, Y_k ($k = 0, \ldots, \text{floor}\,\big(\frac{N-1}{2}\big)$) to obtain consistent estimates of the system parameters. $\Diamond$

Some useful formulas and results about the DFT are reported in Appendix A.

For the following, it is convenient to introduce the parameter vector

$$\boldsymbol{\theta} = \big(a_1 \;\cdots\; a_{n_a} \;\; b_0 \;\cdots\; b_{n_b}\,\big)^T \tag{9}$$

and use the following conventions:

True parameters	$\boldsymbol{\theta}_0$, λ_u^0, λ_y^0, etc
General parameters	$\boldsymbol{\theta}$, λ_u, λ_y, etc
Estimated parameters	$\hat{\boldsymbol{\theta}}$, $\hat{\lambda}_u$, $\hat{\lambda}_y$, etc

3 The frequency domain model

The transfer function of (1) is represented as

$$G(e^{-j\omega}) = \frac{B(e^{-j\omega})}{A(e^{-j\omega})}. \tag{10}$$

With reference to the noise free signals $u_0(t)$ and $y_0(t)$, consider the corresponding DFTs as in (5) and (6). It is a well–known fact, see Pintelon *et al.* (1997), that for finite N, even in absence of noise, the ratio of the DFTs $Y_0(\omega_k)$ and $U_0(\omega_k)$ ($\omega_k = 2\pi k/N$) is not equal to the true transfer function $G(e^{-j\omega_k}) \neq Y_0(\omega_k)/U_0(\omega_k)$. Rather, it can be proved that the DFTs $Y_0(\omega_k)$ and $U_0(\omega_k)$ exactly satisfy an extended model that includes also a transient term, i.e.

$$A(e^{-j\omega_k})\, Y_0(\omega_k) = B(e^{-j\omega_k})\, U_0(\omega_k) + T(e^{-j\omega_k}) \;, \tag{11}$$

where $T(z^{-1})$ is a polynomial of order $n-1$

$$T(z^{-1}) = \tau_0 + \tau_1\, z^{-1} + \cdots + \tau_{n-1}\, z^{-n+1} \quad n = \max\,(n_a, n_b) \tag{12}$$

that takes into account the effects of the initial and final conditions of the experiment. Thus, for the subsequent analysis introduce also the parameter vector

$$\boldsymbol{\vartheta} = \begin{pmatrix} \tau_0 & \cdots & \tau_{n-1} \end{pmatrix}^T . \tag{13}$$

Now introduce the following notations

$$\mathbf{U} = \begin{pmatrix} U_0, U_1, \cdots, U_M \end{pmatrix}^T, \tag{14}$$

$$\mathbf{Y} = \begin{pmatrix} Y_0, Y_1, \cdots, Y_M \end{pmatrix}^T, \tag{15}$$

and let $\mathbf{U}_0$, $\mathbf{Y}_0$ be the correspondence to (14)–(15) for the noise–free data. Further, introduce also ($k = 1, \ldots, M$)

$$A_k = A(\mathrm{e}^{-j\omega_k}),\ B_k = B(\mathrm{e}^{-j\omega_k}),\ T_k = T(\mathrm{e}^{-j\omega_k}), \tag{16}$$

$$G_k = B(\mathrm{e}^{-j\omega_k})/A(\mathrm{e}^{-j\omega_k}), \tag{17}$$

$$H_k = T(\mathrm{e}^{-j\omega_k})/A(\mathrm{e}^{-j\omega_k}), \tag{18}$$

and

$$\mathbf{G} = \operatorname{diag}\big(G_0, G_1, \ldots, G_M\big), \tag{19}$$

$$\mathbf{H} = \begin{pmatrix} H_0, H_1, \cdots, H_M \end{pmatrix}^T . \tag{20}$$

For the noise–free data, for an arbitrary frequency ω_k relation (11) holds, i.e.

$$A_k Y_k^0 = B_k U_k^0 + T_k . \tag{21}$$

For all the frequencies, the system model can be written as

$$\mathbf{Y}_0 = \mathbf{G}\mathbf{U}_0 + \mathbf{H} . \tag{22}$$

In the noisy case it holds instead

$$\mathbf{Y} = \mathbf{G}\mathbf{U}_0 + \mathbf{H} + \tilde{\mathbf{Y}}, \tag{23}$$

$$\mathbf{U} = \mathbf{U}_0 + \tilde{\mathbf{U}}, \tag{24}$$

where the noise vectors $\tilde{\mathbf{Y}}$ and $\tilde{\mathbf{U}}$ are defined in similar way to (14)–(15). Because of Assumptions A5 and A7, they are jointly complex Gaussian distributed. In fact,

$$\begin{pmatrix} \mathbf{Y} \\ \mathbf{U} \end{pmatrix} \sim \mathcal{CN}\left(\begin{pmatrix} \mathbf{G}\mathbf{U}_0 + \mathbf{H} \\ \mathbf{U}_0 \end{pmatrix}, \begin{pmatrix} \rho\lambda_u \mathbf{I} & \mathbf{0} \\ \mathbf{0} & \lambda_u \mathbf{I} \end{pmatrix} \right) . \tag{25}$$

where the identity matrices in (25) are of dimension $M \times M$.

The unknown quantities in the model (25) are:

- The parameter vector $\boldsymbol{\theta}$, which enters in $\mathbf{G}$ and $\mathbf{H}$,
- The input noise variance λ_u,
- The auxiliary parameter vector $\boldsymbol{\vartheta}$, which enters in $\mathbf{H}$. In particular, note that $\mathbf{H}$ depends *linearly* on $\boldsymbol{\vartheta}$.
- The noise-free data vector $\mathbf{U}_0$.

Remark 3.1 *The model (25) is* valid for any set *of frequency values, even for M smaller than* floor $\big(N/2\big)$. *When $M <$* floor $\big(N/2\big)$ *one is effectively low-pass filtering the data.*

4 The frequency domain ML estimator

Using the model (25), one can directly set up the likelihood function, cf. Söderström (2002). Use the pdf of complex-valued circular Gaussian variables. The result will be

$$\begin{aligned}\log(L) &= -(\mathbf{Y}-\mathbf{G}\mathbf{U}_0-\mathbf{H})^*(\mathbf{Y}-\mathbf{G}\mathbf{U}_0-\mathbf{H})/(\rho\lambda_u) \\ &\quad -(\mathbf{U}-\mathbf{U}_0)^*(\mathbf{U}-\mathbf{U}_0)/\lambda_u \\ &\quad -\log(\det(\rho\lambda_u\mathbf{I}))-\log(\det(\lambda_u\mathbf{I})), \end{aligned} \tag{26}$$

where L is the likelihood function. The maximum likelihood estimates of the unknowns $\boldsymbol{\theta},\ \lambda_u,\ \boldsymbol{\vartheta}$ and $\mathbf{U}_0$ are

$$\hat{\boldsymbol{\theta}}, \hat{\lambda}_u, \hat{\boldsymbol{\vartheta}}, \hat{\mathbf{U}}_0 = \arg \min_{\boldsymbol{\theta},\lambda_u,\boldsymbol{\vartheta},\mathbf{U}_0} -\log(L)\,. \tag{27}$$

To derive the ML estimator, one has to find a way to express the maximum point of the likelihood function, with respect to all the unknowns. Fortunately, this is a separable nonlinear least squares problem, which allows the maximization to be done with respect to the different unknowns to be treated in separate steps. Next the details are developed.

4.1 Maximization with respect to λ_u

First consider how the likelihood function L depends on the unknown λ_u. Rewrite (26) as

$$\log(L) = -V_1/\lambda_u - \log(\rho^M\lambda_u^M) - \log(\lambda_u^M) \tag{28}$$

$$\begin{aligned}V_1(\boldsymbol{\theta},\mathbf{U}_0,\boldsymbol{\vartheta}) &\triangleq (\mathbf{Y}-\mathbf{G}\mathbf{U}_0-\mathbf{H})^*(\mathbf{Y}-\mathbf{G}\mathbf{U}_0-\mathbf{H})/\rho \\ &\quad +(\mathbf{U}-\mathbf{U}_0)^*(\mathbf{U}-\mathbf{U}_0). \end{aligned} \tag{29}$$

Maximization of L with respect to λ_u is now straightforward. Direct differentiation gives

$$0 = \frac{\partial \log(L)}{\partial \lambda_u} = V_1/\lambda_u^2 - 2M/\lambda_u, \tag{30}$$

and hence the maximizing argument for λ_u is

$$\hat{\lambda}_u = \frac{1}{2M}\min_{\boldsymbol{\theta},\mathbf{U}_0,\boldsymbol{\vartheta}} V_1 = \frac{1}{2M}V_1(\hat{\boldsymbol{\theta}},\hat{\mathbf{U}}_0,\hat{\boldsymbol{\vartheta}})\,. \tag{31}$$

The conclusion so far is that to maximize the likelihood function, one needs to find the minimum point of the criterion V_1 with respect to $\boldsymbol{\theta}, \mathbf{U}_0, \boldsymbol{\vartheta}$.

4.2 Minimization with respect to $\mathbf{U}_0$

Note that the loss function $V_1(\boldsymbol{\theta}, \mathbf{U}_0, \boldsymbol{\vartheta})$ is quadratic in $\mathbf{U}_0$, see (29). Hence this minimization is straightforward. It holds

$$\begin{aligned} V_1(\boldsymbol{\theta}, \mathbf{U}_0, \boldsymbol{\vartheta}) \quad = \quad & \mathbf{U}_0^* \left[\mathbf{G}^*\mathbf{G}/\rho + \mathbf{I}\right] \mathbf{U}_0 \\ & - \mathbf{U}_0^* \left[\mathbf{G}^*(\mathbf{Y} - \mathbf{H})/\rho + \mathbf{U}\right] \\ & - \left[(\mathbf{Y}^* - \mathbf{H}^*)\mathbf{G}/\rho + \mathbf{U}^*\right] \mathbf{U}_0 \\ & + (\mathbf{Y}^* - \mathbf{H}^*)(\mathbf{Y} - \mathbf{H})/\rho + \mathbf{U}^*\mathbf{U}\,, \end{aligned} \tag{32}$$

so the minimizing argument is

$$\hat{\mathbf{U}}_0 = \left[\hat{\mathbf{G}}^*\hat{\mathbf{G}}/\rho + \mathbf{I}\right]^{-1} \left[\hat{\mathbf{G}}^*(\mathbf{Y} - \hat{\mathbf{H}})/\rho + \mathbf{U}\right], \tag{33}$$

and the minimal value of the loss function is

$$\begin{aligned} V_2(\boldsymbol{\theta}, \boldsymbol{\vartheta}) \quad & \triangleq \quad \min_{\mathbf{U}_0} V_1(\boldsymbol{\theta}, \mathbf{U}_0, \boldsymbol{\vartheta}) \\ & = \quad (\mathbf{Y}^* - \mathbf{H}^*)(\mathbf{Y} - \mathbf{H})/\rho + \mathbf{U}^*\mathbf{U} \\ & \qquad - \left[(\mathbf{Y}^* - \mathbf{H}^*)\mathbf{G}/\rho + \mathbf{U}^*\right] \left[\mathbf{G}^*\mathbf{G}/\rho + \mathbf{I}\right]^{-1} \\ & \qquad \times \left[\mathbf{G}^*(\mathbf{Y} - \mathbf{H})/\rho + \mathbf{U}\right] . \end{aligned} \tag{34}$$

It also follows that, see (31),

$$\hat{\lambda}_u = \frac{1}{2M} V_2(\hat{\boldsymbol{\theta}}, \hat{\boldsymbol{\vartheta}})\,. \tag{35}$$

4.3 Minimization with respect to $\boldsymbol{\vartheta}$

Next proceed and minimize $V_2(\boldsymbol{\theta}, \boldsymbol{\vartheta})$ with respect to $\boldsymbol{\vartheta}$. The key observation is then to note that V_2 is a quadratic function of $\mathbf{H}$, and that $\mathbf{H}$ depends linearly on $\boldsymbol{\vartheta}$. From (12), (13), (18) and (20) one can write

$$\mathbf{H} \quad = \quad \mathbf{K}\boldsymbol{\vartheta}, \tag{36}$$

$$\mathbf{K} \quad = \quad \begin{pmatrix} \frac{1}{A_0} \mathrm{e}^{-j\omega_0(n-1)} & \dots & \frac{1}{A_0} \\ \vdots & & \vdots \\ \frac{1}{A_{M-1}} \mathrm{e}^{-j\omega_{M-1}(n-1)} & \dots & \frac{1}{A_{M-1}} \end{pmatrix} \triangleq \begin{pmatrix} \mathbf{k}_0 \\ \vdots \\ \mathbf{k}_{M-1} \end{pmatrix} . \tag{37}$$

Inserting (36) into (34) gives

$$\begin{aligned} V_2(\,\boldsymbol{\theta}, \boldsymbol{\vartheta}) \;=\; & \boldsymbol{\vartheta}^T \Big(\mathbf{K}^*\mathbf{K}/\rho - \mathbf{K}^*\mathbf{G}\rho \left[\mathbf{G}^*\mathbf{G}/\rho + \mathbf{I}\right]^{-1} \\ & \times\, \mathbf{G}^*\mathbf{K}/\rho \Big) \boldsymbol{\vartheta} \\ & + \boldsymbol{\vartheta}^T \Big(-\mathbf{K}^*\mathbf{Y}/\rho + \mathbf{K}^*\mathbf{G}/\rho \left[\mathbf{G}^*\mathbf{G}/\rho + \mathbf{I}\right]^{-1} \\ & \times\, (\mathbf{G}^*\mathbf{Y}/\rho + \mathbf{U}) \Big) \\ & + \Big((\mathbf{Y}^*\mathbf{G}/\rho + \mathbf{U}^*) \left[\mathbf{G}^*\mathbf{G}/\rho + \mathbf{I}\right]^{-1} \mathbf{G}^*\mathbf{K}/\rho \\ & - \mathbf{Y}^*\mathbf{K}/\rho \Big) \boldsymbol{\vartheta} \\ & + \mathbf{Y}^*\mathbf{Y}/\rho + \mathbf{U}^*\mathbf{U} - (\mathbf{Y}^*\mathbf{G}/\rho + \mathbf{U}^*) \\ & \times \left[\mathbf{G}^*\mathbf{G}/\rho + \mathbf{I}\right]^{-1} (\mathbf{G}^*\mathbf{Y}/\rho + \mathbf{U})\;. \end{aligned} \tag{38}$$

It is seen that the argument $\boldsymbol{\vartheta}$ that minimizes $V_2(\boldsymbol{\theta}, \boldsymbol{\vartheta})$ is given by

$$\begin{aligned} \hat{\boldsymbol{\vartheta}} \;=\; & \Big(\hat{\mathbf{K}}^*\hat{\mathbf{K}}/\rho - \hat{\mathbf{K}}^*\hat{\mathbf{G}}\rho \left[\hat{\mathbf{G}}^*\hat{\mathbf{G}}/\rho + \mathbf{I}\right]^{-1} \hat{\mathbf{G}}^*\hat{\mathbf{K}}/\rho \Big)^{-1} \\ & \times \Big(-\hat{\mathbf{K}}^*\mathbf{Y}/\rho + \hat{\mathbf{K}}^*\hat{\mathbf{G}}/\rho \left[\hat{\mathbf{G}}^*\hat{\mathbf{G}}/\rho + \mathbf{I}\right]^{-1} \\ & \times\, \Big(\hat{\mathbf{G}}^*\mathbf{Y}/\rho + \mathbf{U} \Big) \Big)\;, \end{aligned} \tag{39}$$

while the minimal value is

$$\min_{\boldsymbol{\theta}, \boldsymbol{\vartheta}} V_2(\boldsymbol{\theta}, \boldsymbol{\vartheta}) \;=\; V_2(\hat{\boldsymbol{\theta}}, \hat{\boldsymbol{\vartheta}}) = M V_3(\hat{\boldsymbol{\theta}}), \tag{40}$$

$$\hat{\boldsymbol{\theta}} \;=\; \arg\min_{\boldsymbol{\theta}} V_3(\boldsymbol{\theta}), \tag{41}$$

$$\begin{aligned} V_3(\boldsymbol{\theta}) \;\triangleq\; & \frac{1}{M} \left[\mathbf{Y}^*\mathbf{Y}/\rho + \mathbf{U}^*\mathbf{U}\right] \\ & - \frac{1}{M} (\mathbf{Y}^*\mathbf{G}/\rho + \mathbf{U}^*) \left[\mathbf{G}^*\mathbf{G}/\rho + \mathbf{I}\right]^{-1} (\mathbf{G}^*\mathbf{Y}/\rho + \mathbf{U}) \\ & - \frac{1}{M} \Big((\mathbf{Y}^*\mathbf{G}/\rho + \mathbf{U}^*) \\ & \times\, \left[\mathbf{G}^*\mathbf{G}/\rho + \mathbf{I}\right]^{-1} \mathbf{G}^*\mathbf{K}/\rho - \mathbf{Y}^*\mathbf{K}/\rho \Big) \\ & \times \Big(\mathbf{K}^*\mathbf{K}/\rho - \mathbf{K}^*\mathbf{G}/\rho \left[\mathbf{G}^*\mathbf{G}/\rho + \mathbf{I}\right]^{-1} \mathbf{G}^*\mathbf{K}/\rho \Big)^{-1} \\ & \times \Big(-\mathbf{K}^*\mathbf{Y}/\rho + \mathbf{K}^*\mathbf{G}/\rho \left[\mathbf{G}^*\mathbf{G}/\rho + \mathbf{I}\right]^{-1} \\ & \times\, (\mathbf{G}^*\mathbf{Y}/\rho + \mathbf{U}) \Big)\;. \end{aligned} \tag{42}$$

Also, cf. (35),

$$\hat{\lambda}_u = \frac{1}{2} V_3(\hat{\boldsymbol{\theta}})\,. \tag{43}$$

Note that the normalization factor M is inserted in (40), (43) for convenience in the following analysis only.

4.4 Minimization with respect to $\boldsymbol{\theta}$

The result of the calculations so far is that the ML estimate of $\boldsymbol{\theta}$ can be obtained by minimizing the function $V_3(\boldsymbol{\theta})$, in which none of the other originally introduced unknowns appear. In this subsection the expression for the loss function $V_3(\boldsymbol{\theta})$ is rewritten using frequency domain formulas. It is important to recall that the matrix $\mathbf{G}$ is diagonal, see (19). It holds, with all summations being over $\sum_0^{M-1}$,

$$\begin{aligned}
V_3(\boldsymbol{\theta}) \quad = \quad & \frac{1}{M}\left[\frac{1}{\rho}\sum_j |Y_j|^2 + \sum_j |U_j|^2\right] \\
& -\frac{1}{M}\sum_j \frac{|G_j^* Y_j/\rho + U_j|^2}{G_j^* G_j/\rho + 1} \\
& -\frac{1}{M}\left(\sum_j \frac{Y_j^* G_j/\rho + U_j^*}{G_j^* G_j/\rho + 1} G_j^* \mathbf{k}_j/\rho - \sum_j Y_j^* \mathbf{k}_j/\rho\right) \\
& \times\left[\frac{1}{\rho}\sum_j \mathbf{k}_j^* \mathbf{k}_j - \sum_j \frac{\mathbf{k}_j^* G_j}{\rho}\frac{G_j^* \mathbf{k}_j}{\rho}\frac{1}{G_j G_j^*/\rho + 1}\right]^{-1} \\
& \times\left(\sum_j -\mathbf{k}_j^* Y_j/\rho + \sum_j \frac{\mathbf{k}_j^* G_j}{\rho}\frac{G_j^* Y_j/\rho + U_j}{G_j G_j^*/\rho + 1}\right).
\end{aligned} \tag{44}$$

The result (44) can be further rewritten as

$$V_3(\boldsymbol{\theta}) = \frac{1}{M}\sum_j \frac{|Y_j|^2 (G_j G_j^*/\rho + 1) + |U_j|^2 \rho (G_j G_j^*/\rho + 1)}{\rho (G_j G_j^*/\rho + 1)}$$

$$
\begin{aligned}
&- \frac{1}{M}\sum_j \frac{\rho|G_j^* Y_j/\rho + U_j|^2}{\rho(G_jG_j^*/\rho+1)} \\
&- \frac{1}{M}\left(\sum_j \frac{(Y_j^*G_j/\rho + U_j^*)G_j^* - Y_j^*(G_jG_j^*/\rho+1)}{\rho(G_jG_j^*/\rho+1)}\mathbf{k}_j\right) \\
&\quad \times \left(\sum_j \mathbf{k}_j\mathbf{k}_j^* \frac{\rho(G_jG_j^*/\rho+1) - G_jG_j^*}{\rho^2(G_jG_j^*/\rho+1)}\right)^{-1} \\
&\quad \times \left(\sum_j \mathbf{k}_j^* \frac{G_j(G_j^*Y_j/\rho + U_j) - Y_j(G_jG_j^*/\rho+1)}{\rho(G_jG_j^*/\rho+1)}\right) \\
&= \frac{1}{M}\sum_j \frac{Y_jY_j^* + U_jU_j^*G_jG_j^* - G_j^*Y_jU_j^* - G_jY_j^*U_j}{G_jG_j^*+\rho} \\
&- \frac{1}{M}\left(\sum_j \frac{U_j^*G_j^* - Y_j^*}{G_jG_j^*+\rho}\mathbf{k}_j\right)\left(\sum_j \mathbf{k}_j^*\mathbf{k}_j \frac{1}{G_jG_j^*+\rho}\right)^{-1} \\
&\quad \times \left(\sum_j \mathbf{k}_j^* \frac{G_jU_j - Y_j}{G_jG_j^*+\rho}\right) . \qquad (45)
\end{aligned}
$$

The first part (45) can be rewritten as

$$
\begin{aligned}
V_{31}(\boldsymbol{\theta}) &= \frac{1}{M}\sum_{j=0}^{M-1} \frac{|Y_j - B_j/A_jU_j|^2}{|B_j/A_j|^2+\rho} \\
&= \frac{1}{M}\sum_{j=0}^{M-1} \frac{|A_jY_j - B_jU_j|^2}{\rho|A_j|^2+|B_j|^2} . \qquad (46)
\end{aligned}
$$

Remark 4.1 $V_{31}(\boldsymbol{\theta})$ *turns out to be precisely the form of the ML criterion in the frequency domain used as the basis for the SML method, see Schoukens* et al. *(1997). The SML method assumes periodic data, and includes then also estimates of the noise variances, replacing ρ. The second part of (45) corresponds to the effects of the transients, in the computation of the DFT, when the data are finite and not periodic. An interesting point is, at present, to understand whether or not the contribution of the second term is minor compared to the first term. In fact, one would expect its impact to be small compared to that of the first term.*

4.5 The ML Algorithm

The general minimization problem (27) with respect to $\boldsymbol{\theta}, \lambda_u, \boldsymbol{\vartheta}, \mathbf{U}_0$ has been reduced in dimension to optimization over only $\boldsymbol{\theta}$:

$$\hat{\boldsymbol{\theta}} = \arg\min_{\boldsymbol{\theta}} V_3(\boldsymbol{\theta}) \qquad (47)$$

with $V_3(\boldsymbol{\theta})$ given by (42) or equivalently (45). The minimization in (47) has to be carried out using a numerical search algorithm, and will then require an iterative procedure. As for similar optimization problems, this is NP hard, and there is a potential risk for converging to local false minima. It makes sense to start the iterations over $\boldsymbol{\theta}$ using some consistent estimate, for example obtained with the generalized instrumental variable method, Söderström (2011). During the undertaken numerical studies, part of which are reported in Section 6, no practical problems of convergence to false, local minimum points of the criterion $V_3(\boldsymbol{\theta})$ were detected.

Once $\hat{\boldsymbol{\theta}}$ is found, the remaining parameters are found as, cf. (39), (33), (43),

$$
\begin{aligned}
\hat{\boldsymbol{\vartheta}} &= \Big(\hat{\mathbf{K}}^*\hat{\mathbf{K}}/\rho - \hat{\mathbf{K}}^*\hat{\mathbf{G}}\rho \left[\hat{\mathbf{G}}^*\hat{\mathbf{G}}/\rho + \mathbf{I}\right]^{-1} \hat{\mathbf{G}}^*\hat{\mathbf{K}}/\rho\Big)^{-1} \\
&\quad \times \Big(-\hat{\mathbf{K}}^*\mathbf{Y}/\rho + \hat{\mathbf{K}}^*\hat{\mathbf{G}}/\rho \left[\hat{\mathbf{G}}^*\hat{\mathbf{G}}/\rho + \mathbf{I}\right]^{-1} \\
&\quad \times \Big(\hat{\mathbf{G}}^*\mathbf{Y}/\rho + \mathbf{U}\Big)\Big)\,, \qquad (48) \\
\hat{\mathbf{U}}_0 &= \left[\hat{\mathbf{G}}^*\hat{\mathbf{G}}/\rho + \mathbf{I}\right]^{-1} \left[\hat{\mathbf{G}}^*(\mathbf{Y} - \hat{\mathbf{H}})/\rho + \mathbf{U}\right], \qquad (49) \\
\hat{\lambda}_u &= \frac{1}{2} V_3(\hat{\boldsymbol{\theta}})\,. \qquad (50)
\end{aligned}
$$

Remark 4.2 *The ML estimation problem formulated in (26) turns out to have the same algebraic form as the EIV problem for a static linear system where all the latent variables (corresponding to $\mathbf{U}_0$ here) are estimated. Also for such cases it is known that the estimated parameters are consistent, but the estimated noise variance (corresponding to λ_u) is asymptotically off by 50 percent, as in (50), see Lindley (1947). For this reason to achieve consistency the estimate of λ_u must be modified by doubling the result of (50),*

$$\hat{\lambda}_u = V_3(\hat{\boldsymbol{\theta}})\,. \qquad (51)$$

Remark 4.3 *In many other estimation problems, maximum likelihood estimates are consistent, in contrast to (50). A particular aspect here is that as $\mathbf{U}_0$ is included as unknown to be estimated, so that the number of estimates grows as $\sim N$ when the data length N increases. This is in contrast to many 'standard' ML problems, where the number of unknown parameters stay fixed. It is also noted in Zhang* et al. *(2013) that the derivatives of the likelihood function with respect to the noise variances. are non-zero when evaluated for the true parameters. This fact indicates that the noise statistical properties cannot be consistently estimated using the ML approach.*

5 Consistency and accuracy analysis

Assume in this section that $N \to \infty$.

5.1 Consistency

For simplicity assume here that $M = N$ (which can be implemented as $M = N/2$, see Section 2). What happens for the case $M < N$ is discussed in Section 5.3.

One would like to have

$$\hat{\boldsymbol{\theta}} \to \boldsymbol{\theta}_0. \tag{52}$$

It holds

$$\begin{aligned} \lim_{N\to\infty} \hat{\boldsymbol{\theta}} &= \lim_{N\to\infty} \arg\min_{\boldsymbol{\theta}} V_3(\boldsymbol{\theta}) \\ &= \arg\min_{\boldsymbol{\theta}} \lim_{N\to\infty} V_3(\boldsymbol{\theta}), \end{aligned} \tag{53}$$

as the convergence is uniform, see below. Hence, it is needed to check the minimum points of the asymptotic loss function $\lim_{N\to\infty} V_3(\boldsymbol{\theta})$.
For this purpose, split the loss function $V_3(\boldsymbol{\theta})$ introduced in (45) into two parts as

$$V_3(\boldsymbol{\theta}) = V_{31}(\boldsymbol{\theta}) + V_{32}(\boldsymbol{\theta}), \tag{54}$$

where $V_{31}(\boldsymbol{\theta})$ was defined in (46). In Appendix B it is shown that the term $V_{32}(\boldsymbol{\theta})$ has a vanishing impact on $V_3(\boldsymbol{\theta})$ in the asymptotic case when $N \to \infty$. Hence it does not matter as far as consistency is concerned. Still it may have a quite beneficial effect for the finite data case, as it will be shown in the numerical examples, see Section 6.3.

For given A and B, introduce the polynomial $C(q^{-1})$ through the spectral factorization, cf. Söderström (2002),

$$CC^* = \rho AA^* + BB^*. \tag{55}$$

Note that the polynomial C is restricted to have all zeros inside the unit circle, but that it is not monic.

Using (55) and (85) one find that $V_{31}(\boldsymbol{\theta})$ can be written as

$$V_{31}(\boldsymbol{\theta}) = \frac{1}{N}\sum_{t=0}^{N-1} \varepsilon^2(t,\boldsymbol{\theta}), \tag{56}$$

$$\varepsilon(t,\boldsymbol{\theta}) = \frac{1}{C(q^{-1})}x(t), \quad x(t) = A(q^{-1})y(t) - B(q^{-1})u(t). \tag{57}$$

Therefore, $V_{31}(\boldsymbol{\theta})$ converges uniformly, *mutatis mutandis* as for standard PEM identification of an ARMAX model. (For the potentially tricky case with C having a zero on the unit circle, it holds by (55) that both A and B have the same zero. This simplifies the analysis compared to the ARMAX case.)

It is shown in Appendix C that the asymptotic function (letting $N \to \infty$) $V_{31}(\boldsymbol{\theta})$ has a minimum point for $\boldsymbol{\theta} = \boldsymbol{\theta}_0$, which due to (53) implies consistency of the parameter estimates.

5.2 Asymptotic distribution

Also in this subsection assume $M = N$. One can derive the asymptotic covariance matrix of the estimate $\hat{\boldsymbol{\theta}}$ by using a standard trick, leading to

$$\sqrt{N}\left(\hat{\boldsymbol{\theta}} - \boldsymbol{\theta}_0\right) \stackrel{N\to\infty}{\longrightarrow} \mathcal{N}(\mathbf{0}, \mathbf{P}_{\boldsymbol{\theta}}), \tag{58}$$

with

$$\begin{aligned} \mathbf{P}_{\boldsymbol{\theta}} &= \mathbf{P}_1^{-1}\mathbf{P}_2\mathbf{P}_1^{-1}, &(59)\\ \mathbf{P}_1 &= \lim_{N\to\infty} V_{31}^{''}(\boldsymbol{\theta}), &(60)\\ \mathbf{P}_2 &= \lim_{N\to\infty} \mathsf{E}\left\{\left(\sqrt{N}V_{31}^{'}(\boldsymbol{\theta})\right)^T\left(\sqrt{N}V_{31}^{'}(\boldsymbol{\theta})\right)\right\}. &(61) \end{aligned}$$

The purpose of the following is to derive explicit expressions for the matrices $\mathbf{P}_1$, (60) and $\mathbf{P}_2$, (61).

To proceed with the analysis, for shortness write (57) as

$$\varepsilon(t) = \frac{A}{C}y(t) - \frac{B}{C}u(t). \tag{62}$$

Set

$$\psi(t) = \varepsilon'(t, \boldsymbol{\theta}_0) = \frac{\partial\varepsilon}{\partial\boldsymbol{\theta}}(t, \boldsymbol{\theta})_{|\boldsymbol{\theta}=\boldsymbol{\theta}_0}. \tag{63}$$

As $\boldsymbol{\theta}_0$ is a minimum point of $V_3(\boldsymbol{\theta})$ (when $N \to \infty$), it must hold

$$\mathsf{E}\varepsilon(t, \boldsymbol{\theta}_0)\psi(t) = 0. \tag{64}$$

Using (56)-(57) and (64) one gets

$$\begin{aligned} &\lim_{N\to\infty} V_{31}(\boldsymbol{\theta}) = \mathsf{E}\varepsilon^2(t, \boldsymbol{\theta}), &(65)\\ &\lim_{N\to\infty} V_{31}'(\boldsymbol{\theta}_0) = 2\mathsf{E}\varepsilon(t, \boldsymbol{\theta}_0)\psi(t), &(66)\\ \mathbf{P}_1 = &\lim_{N\to\infty} V_{31}''(\boldsymbol{\theta}_0) = 2\mathsf{E}\varepsilon(t, \boldsymbol{\theta}_0)\varepsilon''(t, \boldsymbol{\theta}_0) + 2\mathsf{E}\psi(t)\psi^T(t), &(67)\\ \mathbf{P}_2 = &\lim_{N\to\infty} N\frac{4}{N^2}\,\mathsf{E}\sum_{t=0}^{N-1}\sum_{s=0}^{N-1}\varepsilon(t)\psi(t)\varepsilon(s)\psi^T(s)\\ = &\lim_{N\to\infty}\frac{4}{N}\sum_{t=0}^{N-1}\sum_{s=0}^{N-1}\left[\underbrace{(\mathsf{E}\varepsilon(t)\psi(t))}_{=0}\underbrace{\left(\mathsf{E}\varepsilon(s)\psi^T(s)\right)}_{=0}\right.\\ &+ (\mathsf{E}\varepsilon(t)\varepsilon(s))\left(\mathsf{E}\psi(t)\psi^T(s)\right)\\ &\left.+\ (\mathsf{E}\psi(t)\varepsilon(s))\left(\mathsf{E}\varepsilon(t)\psi^T(s)\right)\right]. &(68) \end{aligned}$$

In (68) the properties of the expectation $\mathsf{E}x_1x_2x_3x_4$ for jointly Gaussian variables are used.

To proceed, the different terms in (68) need to be considered in some detail.

It has followed from earlier calculations, see (108), that for $\boldsymbol{\theta} = \boldsymbol{\theta}_0$, the residuals $\varepsilon(t, \boldsymbol{\theta}_0)$ are indeed white noise and have a constant spectrum. Therefore, the relation

$$\mathsf{E}\varepsilon(t)\varepsilon(s) = \lambda_u^0 \delta_{t,s} \tag{69}$$

follows. Indeed, to spell out details of an explicit proof, let $\tau \geq 0$. It holds

$$\varepsilon(t, \boldsymbol{\theta}_0) = \frac{A}{C}\tilde{y}(t) - \frac{B}{C}\tilde{u}(t), \tag{70}$$

$$\begin{aligned} & \mathsf{E}\varepsilon(t+\tau, \boldsymbol{\theta}_0)\varepsilon(t, \boldsymbol{\theta}_0) \\ = \ & \frac{1}{2\pi}\int_{-\pi}^{\pi} \left[\frac{AA^*\rho\lambda_u^0}{CC^*} + \frac{BB^*\lambda_u^0}{CC^*} \right] \mathrm{e}^{\mathrm{i}\,\omega\tau} d\omega \\ = \ & \lambda_u^0 \frac{1}{2\pi i} \oint z^\tau \frac{dz}{z} = \lambda_u^0 \delta_{\tau,0}. \end{aligned} \tag{71}$$

which means that $\varepsilon(t)$ behaves as white noise.

Using (69) simplifies the second terms in (68).

The double sum of the third terms in (68) can be rewritten as

$$\begin{aligned} & \lim_{N\to\infty} \frac{4}{N} \sum_{t=0}^{N-1}\sum_{s=0}^{N-1} \Big(\mathsf{E}\varepsilon(s)\psi(t)\Big) \Big(\mathsf{E}\varepsilon(t)\psi^T(s)\Big) \\ = \ & \lim_{N\to\infty} \frac{4}{N} \sum_{\tau=-N+1}^{N-1} \Big(N - |\tau| \Big) \Big(\mathsf{E}\varepsilon(t+\tau)\psi(t)\Big) \\ & \times \Big(\mathsf{E}\varepsilon(t-\tau)\psi^T(t)\Big) \\ = \ & 4 \sum_{\tau=-\infty}^{\infty} \Big(\mathsf{E}\varepsilon(t+\tau)\psi(t)\Big) \Big(\mathsf{E}\varepsilon(t-\tau)\psi^T(t)\Big), \end{aligned} \tag{72}$$

assuming that the cross-covariance $\mathsf{E}\varepsilon(t+\tau)\psi(t)$ is exponentially bounded as a function of τ.

The expressions for $\mathbf{P}_1$ and $\mathbf{P}_2$ therefore run as follows, cf. (67), (68).

$$\mathbf{P}_1 = 2\mathsf{E}\psi(t)\psi^T(t) + 2\mathsf{E}\varepsilon(t, \boldsymbol{\theta}_0)\varepsilon''(t, \boldsymbol{\theta}_0), \tag{73}$$

$$\begin{aligned} \mathbf{P}_2 = \ & 4\lambda_u^0 \mathsf{E}\psi(t)\psi^T(t) \\ & +4 \sum_{\tau=-\infty}^{\infty} \left(\mathsf{E}\varepsilon(t+\tau)\psi(t)\right) \left(\mathsf{E}\varepsilon(t-\tau)\psi^T(t)\right). \end{aligned} \tag{74}$$

It is clear from the previous analysis, that for the EIV case all terms in (73), (74) must be taken into account, and none can be assumed to be identically zero. It remains to develop some algorithm for how to compute these additional terms.

Algorithmic details, based on the development in this section, for how to compute $\mathbf{P}_{\boldsymbol{\theta}}$ are given in Appendix D.

Remark 5.1 *Equation (56) happens to be the same type of expression as for the ML estimation of ARMA processes with all polynomial coefficients as unknowns. However, in the ARMA case $\varepsilon(t, \boldsymbol{\theta}_0)$ is white noise, and the derivative $\partial\varepsilon(t, \boldsymbol{\theta})/\partial\boldsymbol{\theta}$ depends automatically only on past values of the measured data, and thereby on past values of $\varepsilon(t, \boldsymbol{\theta})$. It turns out that this does not apply in the EIV case. As a consequence, the expressions for $\mathbf{P}_1$ and $\mathbf{P}_2$ become more complicated, with no zero terms in (73), (74).*

Finally, one can derive the asymptotic covariance matrix of the extended vector $\begin{pmatrix} \boldsymbol{\theta}^T & \lambda_u \end{pmatrix}^T$. Referring to the analysis for the pure ARMA case, the result appears to be, *mutatis mutandis*,

$$\sqrt{N}\left(\begin{pmatrix} \hat{\boldsymbol{\theta}} \\ \hat{\lambda}_u \end{pmatrix} - \begin{pmatrix} \boldsymbol{\theta}_0 \\ \lambda_u^0 \end{pmatrix}\right) \overset{N\to\infty}{\longrightarrow} \mathcal{N}(\begin{pmatrix} \mathbf{0} \\ \mathbf{0} \end{pmatrix}, \begin{pmatrix} \mathbf{P}_{\boldsymbol{\theta}} & \mathbf{0} \\ \mathbf{0} & 2\lambda_u^2 \end{pmatrix}), \tag{75}$$

cf. Ljung (1999), Söderström and Stoica (1989).

5.3 The case $M < N$

The analysis so far in Section 5 was done under the assumption $M = N$. In this subsection it is analyzed what happens if instead $M < N$, which is a way of using low-pass filtered data. Set $\alpha = M/N, 0 < \alpha \leq 1$.

Consider first the consistency aspects. Instead of (105) one gets now, see also (95)

$$\begin{aligned} V_{31}(\boldsymbol{\theta}) &= \frac{1}{M}\sum_{j=0}^{M-1}\frac{|X_j|^2}{|C_j|^2} \\ &\to \frac{1}{\alpha}\frac{1}{2\pi}\int_{-\alpha\pi}^{\alpha\pi}\phi_\varepsilon(\omega)d\omega \\ &= \frac{1}{\alpha}\frac{1}{2\pi}\int_{-\alpha\pi}^{\alpha\pi}\frac{|AB_0 - AB_0|^2}{|A_0C|^2}\phi_{u_0}(\omega)d\omega \\ &\quad + \frac{1}{\alpha}\frac{1}{2\pi}\int_{-\alpha\pi}^{\alpha\pi}\lambda_u d\omega. \end{aligned} \tag{76}$$

Cf. (107). Apparently consistency still applies, as $\boldsymbol{\theta} = \boldsymbol{\theta}_0$ is the unique minimum point of $V_{31}(\boldsymbol{\theta})$ as soon as the input spectrum $\phi_{u_0}(\omega)$ is strictly positive for at least $n_a + n_b + 1$ distinct frequencies in the interval $[0, \alpha 2\pi]$.

Next consider the accuracy properties. The expressions (59)-(61) still apply. To proceed, one may write

$$\begin{aligned} V_{31}(\boldsymbol{\theta}) &= \frac{1}{M}\sum_{j=0}^{M-1}\frac{|X_j|^2}{|C_j|^2} = \frac{1}{\alpha}\frac{1}{N}\sum_{j=0}^{M-1}\frac{|X_{\alpha j}|^2}{|C_j|^2} \\ &= \frac{1}{\alpha N}\sum_{t=0}^{N-1}\left[\frac{F_\alpha}{C}\left(Ay(t) - Bu(t)\right)\right]^2. \end{aligned} \tag{77}$$

The differences as compared to the case $M = N$ treated in some detail in Section 6.2 are to account for the scaling factor $1/\alpha$ and the ideal low-pass filter F_α. The details for how to do this are omitted.

6 Numerical examples

In the following three subsection we illustrate some different aspects of the estimator.

6.1 The asymptotic covariance matrix

In this subsection the ML estimator is compared to some other methods, and its asymptotic performance is compared to the theoretical findings in Subsection 5.2.

A Monte Carlo study with the noise-free input being an AR process

$$(1 + d_1 q^{-1} + d_2 q^{-2}) u_0(t) = v(t), \tag{78}$$

$d_1 = -0.25, d_2 = 0.9$, was undertaken. The signal-to-noise ratio was 10 on both the input and the output side. $N = 10000$ data points and $N_{\text{sim}} = 500$ realizations were used. The weakly damped second order system

$$(1 - 1.3q^{-1} + 0.94q^{-2}) y_0(t) = (0.7 + 0.35q^{-1}) u_0(t) \tag{79}$$

was used. For comparison, some other estimators were applied as well:

- The prediction error method (PEM) was applied using a second order ARMAX model. Note that

  $$A(q^{-1})y(t) - B(q^{-1})u(t) = A(q^{-1})\tilde{y}(t) - B(q^{-1})\tilde{u}(t)$$

  and the right hand side behaves as an MA process, and can be written as $C(q^{-1})\varepsilon(t)$. A closer analysis shows though that $\varepsilon(t)$ is correlated with future values of $u(t)$, which corresponds to the presence of a non-causal feedback, see Söderström *et al.* (2002). This fact prevents consistency.

- The total least squares (TLS) method. In system identification it is also known as the Koopman-Levin method, see Fernando and Nicholson (1985). The TLS method is known to give consistency only when $\lambda_u = \lambda_y$, or equivalently, when the noise variance ratio ρ is known and the signals are appropriate scaled. It thus shares the use of Assumption A7 with the ML method studied here.

- The generalized instrumental variable (GIVE) method, Söderström (2011). In this case the instrumental vector is chosen to consist of $y(t), \ldots, y(t-3), u(t), \ldots, u(t-2)$.

The results are presented in Table 1. The results are very reasonable. The theoretical variance expression $\mathbf{P}_{\boldsymbol{\theta}}$ coincides well with the result of the MC simulations. As expected the PEM estimates have a considerable bias. The ML estimates are more accurate than those produced by TLS and GIVE.

6.2 The effect of M

To study the effect of M, the same system as in Section 6.1 was studied. Two cases, using different resonant AR(2) processes (78) as noise-free input, was considered. In both cases the signal-to-noise ratio was 10 at the input and at the output side.

Table 1: Parameter estimates and standard deviations

Parameter	True value	PEM	TLS	GIVE	ML	Theor. std (ML)
a_1	-1.3	-1.2750 ± 0.0033	-1.3003 ± 0.0039	-1.3000 ± 0.0036	-1.3000 ± 0.0028	0.0026
a_2	0.94	0.9232 ± 0.0029	0.9404 ± 0.0040	0.9399 ± 0.0036	0.9399 ± 0.0027	0.0027
b_0	0.7	0.5922 ± 0.0067	0.7007 ± 0.0099	0.7000 ± 0.0091	0.7002 ± 0.0066	0.0066
b_1	0.35	0.3019 ± 0.0070	0.3494 ± 0.0097	0.3500 ± 0.0096	0.3503 ± 0.0070	0.0067
λ_u	0.7713	-	0.7702 ± 0.0154	0.7691 ± 0.0660	0.7720 ± 0.0114	0.0109

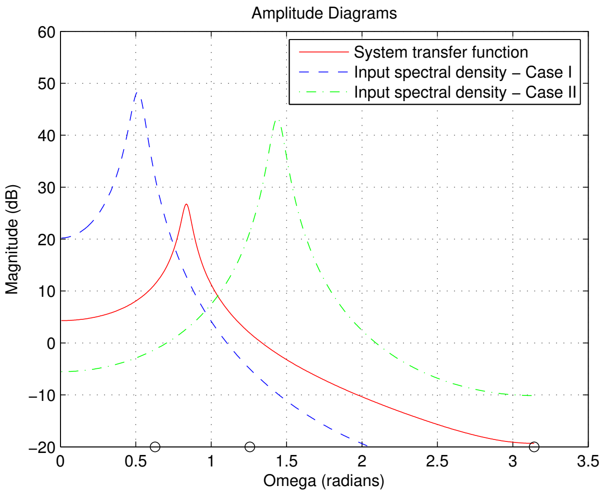

Figure 2: The frequency contents of the system transfer function (solid line), input spectral density (case I dashed line; case II dashdotted line) Both $\alpha = 0.5$ and $\alpha = 1$ correspond to the circle at $\omega = \pi$.

Case I: $d_1 = -1.65, d_2 = 0.9$.
Case II: $d_1 = -0.25, d_2 = 0.9$.

In Figure 2 the transfer function of the system as well as the power spectra of the two AR processes are illustrated.

The system was identified using Monte Carlo studies for some different values of α. These α values are also displayed as circles on the frequency axis in Figure 2, noting that the corresponding angular frequency is $2\pi\alpha$. The results obtained are shown in Table 2. The theoretical standard deviations were computed using (75). If $\alpha \leq 0.5$, N was substituted by $M = \alpha N$, as a smaller number of terms were then used in (43), (46). As in Section 6.1, $N = 10000$, $N_{\text{sim}} = 500$.

Some observations:

- The results for $\alpha = 0.5$ and $\alpha = 1$ are almost the same, for both cases, as predicted by the theory, see Section 2.

Table 2: Monte Carlo studies for different values of $\alpha = M/N$. The table displays arithmetic means and standard deviations. The theoretical standard deviations do not depend on α.

Parameter	True value	α	Case I	Theor. std Case I	Case II	Theor. std Case II
a_1	-1.3	0.1	-1.2984 ± 0.0267		-1.3220 ± 0.2037	
		0.2	-1.3000 ± 0.0023		-1.2999 ± 0.0029	
		0.5	-1.3000 ± 0.0024		-1.2999 ± 0.0027	
		1	-1.3000 ± 0.0024	0.0021	-1.2999 ± 0.0027	0.0026
a_2	0.94	0.1	0.9388 ± 0.0338		0.9682 ± 0.2846	
		0.2	0.9399 ± 0.0022		0.9397 ± 0.0029	
		0.5	0.9399 ± 0.0022		0.9398 ± 0.0028	
		1	0.9399 ± 0.0022	0.0021	0.9398 ± 0.0028	0.0027
b_0	0.7	0.1	0.7048 ± 0.0825		0.6286 ± 0.6755	
		0.2	0.7012 ± 0.0119		0.7002 ± 0.0165	
		0.5	0.7011 ± 0.0120		0.7001 ± 0.0070	
		1	0.7011 ± 0.0120	0.0113	0.7001 ± 0.0070	0.0066
b_1	0.35	0.1	0.3470 ± 0.0993		0.4316 ± 0.8276	
		0.2	0.3490 ± 0.0132		0.3507 ± 0.0176	
		0.5	0.3491 ± 0.0135		0.3505 ± 0.0069	
		1	0.3491 ± 0.0135	0.0123	0.3505 ± 0.0069	0.0067
λ_u	1	0.1	0.9985 ± 0.0320		0.9983 ± 0.0305	
		0.2	1.0024 ± 0.0236		1.0017 ± 0.0217	
		0.5	1.0012 ± 0.0141		1.0008 ± 0.0151	
		1	1.0013 ± 0.0141	0.0141	1.0008 ± 0.0151	0.0141

- The system has its main amplification within the frequency interval $[0.1 - 0.2] \times 2\pi$.
- For Case I the noise-free input has the dominating part of its energy below the angular frequency $0.1 \times 2\pi$, cf. Figure 2. The estimation results are essentially the same in Table 2 when $\alpha \geq 0.2$. For all $\alpha \geq 0.2$ the accuracy of the parameters is well predicted by the theory. There is a considerable degradation when $\alpha = 0.1$ (corresponding to a frequency region with low gain in the system).
- For Case II the input has very little of its energy below the angular frequency $0.2 \times 2\pi$. Similarly, the accuracy of the parameter estimates improves considerably when α is increased from 0.1 or 0.2 to 0.5. The degradation of the parameter estimates for $\alpha = 0.1$ is much more pronounced than in Case I. In fact, the frequency region corresponding to $\alpha \leq 0.1$ is much more excited in Case I than in Case II.

6.3 The effect of estimating ϑ

In Section 5.1 has been shown that the loss function $V_3(\boldsymbol{\theta})$ can be split into two terms

$$V_3(\boldsymbol{\theta}) = V_{31}(\boldsymbol{\theta}) + V_{32}(\boldsymbol{\theta}), \tag{80}$$

where $V_{32}(\boldsymbol{\theta})$ has a vanishing impact on $V_3(\boldsymbol{\theta})$ when $N \to \infty$. The goal of the numerical simulations proposed in this subsection is the analysis of the effect of the term $V_{32}(\boldsymbol{\theta})$ for the finite data case.

In this case the system is given by

$$\begin{aligned} A(q^{-1}) &= 1 - 1.5q^{-1} + 0.7q^{-2} \\ B(q^{-1}) &= 2 - 1.0q^{-1} + 0.5q^{-2} \end{aligned} \tag{81}$$

and the noise-free input was an ARMA(1,1) process:

$$(1 - 0.5q^{-1})u_0(t) = (1 + 0.5q^{-1})v(t) \tag{82}$$

The noise variances were chosen so that the SNR was the same at the input and output sides. Three values were considered: SNR = 10 dB, 20 dB and 30 dB.

Estimates were computed in a Monte Carlo study using the loss functions $V_3(\boldsymbol{\theta})$, see eq. (45), and $V_{31}(\boldsymbol{\theta})$, see eq. (46). The number of data points were varied over some powers of 2, more specifically from $N = 256$ to $N = 8192$. 100 independent runs were been performed. The identification procedure has been performed by using only $N/2$ data, i.e with $\alpha = 0.5$. The accuracy of the parameter estimates were the normalized root mean square error

$$\text{NRMSE} = \frac{1}{||\boldsymbol{\theta}||} \sqrt{\frac{1}{100} \sum_{i=1}^{100} ||\hat{\boldsymbol{\theta}}^i - \boldsymbol{\theta}||^2}, \tag{83}$$

where $\hat{\boldsymbol{\theta}}^i$ denotes the estimate of $\boldsymbol{\theta}$ obtained in the i–th trial of the Monte Carlo simulation.

Figure 3 reports the NRMSE versus the number of frequencies N, obtained by using $V_3(\boldsymbol{\theta})$ and $V_{31}(\boldsymbol{\theta})$ for SNR = 20 dB. It can be observed that the influence of the term $V_{32}(\boldsymbol{\theta})$ is evident for low values of N, say until $N < 2048$. In fact, for small N, the two NRMSE values differ substantially. When $N \geq 2048$ the effect of the term $V_{32}(\boldsymbol{\theta})$ is hardly visible. It must be observed that this effect is more evident for high SNR conditions, as illustrated by the results proposed in Figure 4, that makes reference to the case corresponding to a SNR of 30 dB on both input and output.

On the contrary, reducing the SNR, the amount of noise on the data increases. This fact has the twofold effect of reducing the quality of the estimates and shading the effect of the transient term $V_{32}(\boldsymbol{\theta})$. This property is illustrated by the results proposed in Figure 5, referring to the case that corresponds to a SNR = 10 dB on both input and output. The bad effect of the transient term $V_{32}(\boldsymbol{\theta})$ becomes more evident with reference to the estimates of the noise variances λ_u, λ_y. Recall that the estimate of λ_u coincides with the minimum of the loss function $V_3(\boldsymbol{\theta})$, (51). It is not infrequent the case where, for low values of N, the estimates of λ_u and $\lambda_y = \rho\,\lambda_u$ obtained with $V_{31}(\boldsymbol{\theta})$ are quite bad, even if the parameter estimates are still good.

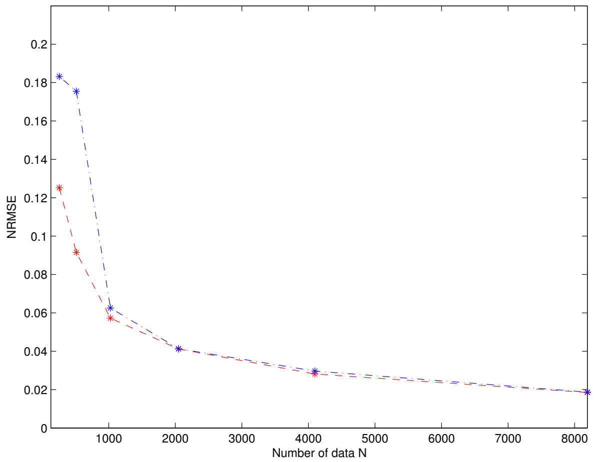

Figure 3: NRMSE versus N for $V_3(\boldsymbol{\theta})$ (red, dashed) and $V_{31}(\boldsymbol{\theta})$ (blue, dash–dotted) - SNR=20 dB.

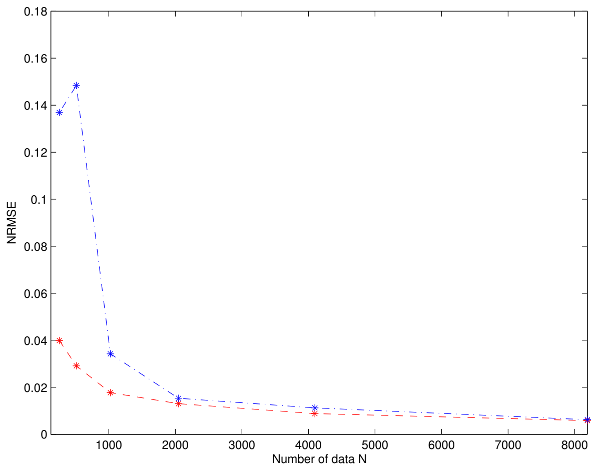

Figure 4: NRMSE versus N for $V_3(\boldsymbol{\theta})$ (red, dashed) and $V_{31}(\boldsymbol{\theta})$ (blue, dash–dotted) - SNR=30 dB.

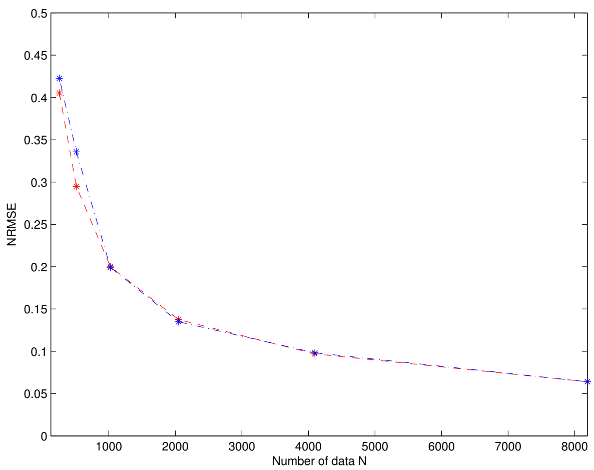

Figure 5: NRMSE versus N for $V_3(\boldsymbol{\theta})$ (red, dashed) and $V_{31}(\boldsymbol{\theta})$ (blue, dash–dotted) - SNR=10 dB.

7 Conclusions

A maximum likelihood approach for the errors-in-variables problem was formulated. Explicit algorithms were derived and analyzed. A basic assumption is that the input and output noises are both white, and has a known variance ratio. The noise-free input is completely arbitrary, and its values are treated as auxiliary parameters.

In particular, the asymptotic distribution of the parameter estimates was derived. It was shown how the asymptotic covariance matrix of that distribution can be computed. The theoretical results and the effects of user choices were further illustrated by numerical examples.

A Parseval's formulas and some related results

Parseval's formula. Set

$$\varphi = \mathrm{e}^{-i2\pi/N} \tag{84}$$

For arbitrary signals $x(t)$ and $y(t)$ whose DFT has been defined in (5), it holds

$$\frac{1}{N}\sum_{j=0}^{N-1} X_j Y_j^* = \frac{1}{N}\sum_{t=0}^{N-1} x(t)y(t) \rightarrow \mathsf{E}\left\{x(t)y(t)\right\}. \tag{85}$$

Further, if $y(t)$ is a constant signal, the limit in (85) will be 0.

Remark A.1 *For a general discrete-time stationary process with covariance function* $r(\tau)$ *define the spectral density as*

$$\phi(\omega) = \sum_{\tau=-\infty}^{\infty} r(\tau) \mathrm{e}^{-i\omega\tau} \tag{86}$$

leading to the inverse transformation

$$r(\tau) = \frac{1}{2\pi} \int_{-\pi}^{\pi} \phi(\omega) \mathrm{e}^{i\omega\tau} d\omega. \tag{87}$$

In particular for $\tau = 0$*,*

$$r(0) = \frac{1}{2\pi} \int_{-\pi}^{\pi} \phi(\omega) d\omega. \tag{88}$$

Frequency domain filtering action. Consider also a further generalization of Parseval's relation that concerns the case when a certain proportion of the frequency points are used. More specifically, assume that $0 < \alpha < 1$ is fixed, and set

$$M = \alpha N. \tag{89}$$

Now examine

$$\frac{1}{M} \sum_{j=0}^{M-1} X_j Y_j^* \tag{90}$$

in the asymptotic case when $N \to \infty$. For this purpose introduce the ideal low-pass filter $F_\alpha(q^{-1})$ described by the frequency function

$$F_\alpha(\mathrm{e}^{\mathrm{i}\omega}) = \begin{cases} 1 & 0 \le \omega \le \alpha 2\pi \\ 0 & \alpha 2\pi < \omega \le 2\pi \end{cases} \tag{91}$$

and the filtered signals

$$x_\alpha(t) = F_\alpha(q^{-1}) x(t), \;\; y_\alpha(t) = F_\alpha(q^{-1}) y(t) \tag{92}$$

leading to

$$X_{\alpha j} = \begin{cases} X_j & 0 \le j \le \alpha(N-1) \\ 0 & j > \alpha(N-1) \end{cases} \tag{93}$$

$$Y_{\alpha j} = \begin{cases} Y_j & 0 \le j \le \alpha(N-1) \\ 0 & j > \alpha(N-1) \end{cases} \tag{94}$$

Then it is found that

$$\begin{aligned} \frac{1}{M} \sum_{j=0}^{M-1} X_j Y_j^* &= \frac{1}{M} \sum_{j=0}^{M-1} X_{\alpha j} Y_{\alpha j}^* = \frac{1}{M} \sum_{j=0}^{N-1} X_{\alpha j} Y_{\alpha j}^* \\ &= \frac{N}{M} \frac{1}{N} \sum_{j=0}^{N-1} X_{\alpha j} Y_{\alpha j}^* \to \frac{1}{\alpha} \mathsf{E}\left\{ x_\alpha(t) y_\alpha(t) \right\} \end{aligned}$$

$$
\begin{aligned}
&= \frac{1}{\alpha}\frac{1}{2\pi}\int_{-\pi}^{\pi}\phi_{x_\alpha y_\alpha}(\omega)d\omega \\
&= \frac{1}{\alpha}\frac{1}{2\pi}\int_{-\alpha\pi}^{\alpha\pi}\phi_{xy}(\omega)d\omega. \qquad (95)
\end{aligned}
$$

B Effect of $V_{32}(\boldsymbol{\theta})$

Consider here the second part of the loss function $V_3(\boldsymbol{\theta}) = V_{31}(\boldsymbol{\theta}) + V_{32}(\boldsymbol{\theta})$, see (45), which can be written as

$$V_{32}(\boldsymbol{\theta}) = -\boldsymbol{\alpha}^*\mathbf{P}^{-1}\boldsymbol{\alpha}. \qquad (96)$$

The vector $\boldsymbol{\alpha}$ and the matrix $\mathbf{P}$ are given by

$$
\begin{aligned}
\boldsymbol{\alpha} &= \frac{1}{M}\sum_{j=0}^{M-1}\mathbf{k}_j^*\frac{G_jU_j - Y_j}{G_jG_j^* + \rho}, \qquad (97)\\
\mathbf{P} &= \frac{1}{M}\sum_{j=0}^{M-1}\mathbf{k}_j^*\mathbf{k}_j\frac{1}{G_jG_j^* + \rho}. \qquad (98)
\end{aligned}
$$

Define the vectors

$$\mathbf{m_j} = \mathbf{k_j A_j}. \qquad (99)$$

Using (37),

$$
\begin{aligned}
\mathbf{P} &= \frac{1}{N}\sum_j \mathbf{k}_j^*\mathbf{k}_j\frac{1}{|B_j|^2/|A_j|^2 + \rho}\\
&= \frac{1}{N}\sum_j \mathbf{m}_j^*\mathbf{m}_j\frac{1}{|B_j|^2 + \rho|A_j|^2}\\
&= \sum_j \mathbf{m}_j^*\mathbf{m}_j\frac{1}{|C_j|^2}. \qquad (100)
\end{aligned}
$$

Therefore, it holds that, as $N \to \infty$,

$$\mathbf{P} \to \mathsf{E}\left\{\begin{pmatrix} v(t-1)\\ \vdots \\ v(t-n)\end{pmatrix}\begin{pmatrix} v(t-1) & \ldots & v(t-n)\end{pmatrix}\right\}, \qquad (101)$$

$$v(t) = \frac{1}{C(q^{-1})}e_0(t), \quad \mathsf{E}\left\{e_0(t)e_0(s)\right\} = \delta_{t,s}. \qquad (102)$$

The matrix in (101) is positive definite and bounded.

Set

$$X_j = A_jY_j - B_jU_j \qquad (103)$$

Next examine the factor $\boldsymbol{\alpha}$ in (97). It holds

$$\boldsymbol{\alpha} = \frac{1}{N}\sum_{j=0}^{N-1}\mathbf{m}_j^*\frac{B_jU_j - A_jY_j}{|B_j|^2 + \rho|A_j|^2}$$

$$= \; -\frac{1}{N}\sum_j \mathbf{m}_j^* \frac{X_j}{|C_j|^2} \to \mathbf{0}. \tag{104}$$

This means that, as already expected, the effect of $V_{32}(\boldsymbol{\theta})$ has a vanishing impact on $V_3(\boldsymbol{\theta})$ in the asymptotic case when $N \to \infty$. Still it may have a quite beneficial effect for the finite data case.

C Consistency analysis

Calculations give for the term $V_{31}(\boldsymbol{\theta})$:

$$\begin{aligned} V_{31}(\boldsymbol{\theta}) &= \frac{1}{N}\sum_{j=0}^{N-1} \frac{|X_j|^2}{\rho|A_j|^2 + |B_j|^2} = \frac{1}{N}\sum_j \frac{|X_j|^2}{|C_j|^2} \\ &\to \mathsf{E}\left\{ \left(\frac{1}{C(q^{-1})} x(t) \right) \right\}, \end{aligned} \tag{105}$$

$$\begin{aligned} \frac{1}{C}x(t) &= \frac{1}{C(q^{-1})}\left[A(q^{-1})y(t) - B(q^{-1})u(t)\right] \\ &= \frac{1}{C(q^{-1})}\left[A(q^{-1})\frac{B_0(q^{-1})}{A_0(q^{-1})}u_0(t) - B(q^{-1})u_0(t)\right] \\ &\quad + \frac{A(q^{-1})}{C(q^{-1})}\tilde{y}(t) - \frac{B(q^{-1})}{C(q^{-1})}\tilde{u}(t). \end{aligned} \tag{106}$$

Hence,

$$\begin{aligned} V_{31}(\boldsymbol{\theta}) &= \frac{1}{2\pi}\int_{-\pi}^{\pi} \frac{|AB_0 - A_0B|^2}{|A_0C|^2}\phi_{u_0} d\omega \\ &\quad + \frac{1}{2\pi}\int_{-\pi}^{\pi} \frac{|A|^2}{|C|^2}\rho\lambda_u^0 + \frac{1}{2\pi}\int_{-\pi}^{\pi} \frac{|B|^2}{|C|^2}\lambda_u^0 \\ &= \frac{1}{2\pi}\int_{-\pi}^{\pi} \frac{|AB_0 - A_0B|^2}{|A_0C|^2}\phi_{u_0} d\omega + \lambda_u^0. \end{aligned} \tag{107}$$

Assuming the signal $u_0(t)$ to have strictly positive spectral density, (107) is minimized for the arguments $A = A_0$, $B = B_0$, that is for $\boldsymbol{\theta} = \boldsymbol{\theta}_0$, and it then holds

$$\min_{\boldsymbol{\theta}} V_{31}(\boldsymbol{\theta}) = \lambda_u^0. \tag{108}$$

As, see Appendix B, the part $V_{32}(\boldsymbol{\theta})$ has a vanishing contribution as $N \to \infty$, it follows that in the limiting case $V_{31}(\boldsymbol{\theta})$ and $V_3(\boldsymbol{\theta})$ have a global minimum for $\boldsymbol{\theta} = \boldsymbol{\theta}_0$. This proves consistency.

D The asymptotic covariance matrix of the parameter estimates

To fully describe the matrix $\mathbf{P}_{\boldsymbol{\theta}}$, it is sufficient to have explicit expressions for $\mathbf{P}_1$ and $\mathbf{P}_2$, see (73), (74).

Introduce further the notations

$$\begin{array}{l} A^\mu = \frac{\partial A}{\partial \boldsymbol{\theta}_u}, \;\; B^\mu = \frac{\partial G}{\partial \boldsymbol{\theta}_u}, \;\; C^\mu = \frac{\partial C}{\partial \boldsymbol{\theta}_u}, \\ \mu = 1, \ldots, n_a + n_b + 1. \end{array} \tag{109}$$

To proceed, differentiate (55) to get

$$\rho A^\mu A^* + \rho A A^{*\mu} + B^\mu B^* + B B^{*\mu} = C^\mu C^* + C C^{*\mu} \tag{110}$$

For the second order derivatives, introduce the notation

$$C^{\mu\nu} = \frac{\partial}{\partial \boldsymbol{\theta}_\nu} C^\mu = \frac{\partial^2}{\partial \boldsymbol{\theta}_\nu \partial \boldsymbol{\theta}_\mu} C, \tag{111}$$

and note that $A^{\mu\nu} = 0,\ B^{\mu\nu} = 0$, as A^μ and B^μ by construction are constant polynomials and do not depend on $\boldsymbol{\theta}$. Differentiation of (110) with respect to $\boldsymbol{\theta}_\nu$ gives

$$\begin{aligned} & \rho A^\mu A^{*\nu} + \rho A^\nu A^{*\mu} + B^\mu B^{*\nu} + B^\mu B^{*\nu} \\ = \;& C^{\mu\nu} C^* + C^\nu C^{*\mu} + C^\mu C^{*\nu} + C C^{*\mu\nu}. \end{aligned} \tag{112}$$

Note that (110) and (112) can be seen as linear Diophantine equations for the unknown polynomials C^μ and $C^{\mu\nu}$, respectively. Equating the different powers of z leads to linear systems of equations in the unknown polynomial coefficients of C^μ and $C^{\mu\nu}$.

To compute $\mathbf{P}_1$ and $\mathbf{P}_2$, proceed as follows. First find C by the spectral factorization (55). Next find C^μ by solving the Diophantine equation (110) for $\mu = 1, \ldots, n_a + n_b + 1$, and $C^{\mu\nu}$ by solving the Diophantine equation (112) for $\mu, \nu = 1, \ldots, n_a + n_b + 1$.

Next examine the correlation between $\varepsilon(t)$ and $\psi(s)$, which appears in the third terms of (68). Using equation (62) gives

$$\begin{aligned} \frac{\partial}{\partial \boldsymbol{\theta}_\mu} \varepsilon(t, \boldsymbol{\theta}) &= \frac{A^\mu}{C} y(t) - \frac{B^\mu}{C} u(t) - \frac{C^\mu}{C^2} \left(A y(t) - B u(t) \right), \\ &= \frac{A^\mu C - A C^\mu}{C^2} \left(\frac{B}{A} u_0(t) + \tilde{y}(t) \right) \\ &\quad - \frac{B^\mu C - B C^\mu}{C^2} \big(u_0(t) + \tilde{u}(t) \big) \\ &= \frac{A^\mu B - A B^\mu}{A C} u_0(t) \\ &\quad + \frac{A^\mu C - A C^\mu}{C^2} \tilde{y}(t) - \frac{B^\mu C - B C^\mu}{C^2} \tilde{u}(t). \\ &\triangleq \frac{A^\mu B - A B^\mu}{A C}\, u_0(t) + \frac{\alpha^\mu}{C^2}\, \tilde{y}(t) - \frac{\beta^\mu}{C^2}\, \tilde{u}(t), \end{aligned} \tag{113}$$

By construction the first term is always uncorrelated with $\varepsilon(t + \tau, \boldsymbol{\theta}_0)$ for any value of τ.

Now, let specifically $\tau \geq 0$. Equations (70), (113) lead to

$$\psi_\mu(t) = \mathsf{E} \varepsilon(t + \tau, \boldsymbol{\theta}_0) \frac{\partial}{\partial \boldsymbol{\theta}_\mu} \varepsilon(t, \boldsymbol{\theta}_0)$$

$$
\begin{aligned}
&= \rho\lambda_u \frac{1}{2\pi i}\oint z^{-\tau}\frac{A^*}{C^*}\frac{A^\mu C - AC^\mu}{C^2}\frac{dz}{z} \\
&\quad +\lambda_u \frac{1}{2\pi i}\oint z^{-\tau}\frac{B^*}{C^*}\frac{B^\mu C - BC^\mu}{C^2}\frac{dz}{z}
\end{aligned} \tag{114}
$$

Using (110) in (114) now leads to

$$
\begin{aligned}
&\mathsf{E}\varepsilon(t+\tau,\boldsymbol{\theta}_0)\frac{\partial}{\partial\boldsymbol{\theta}_\mu}\varepsilon(t,\boldsymbol{\theta}_0) \\
&= \lambda_u \frac{1}{2\pi i}\oint z^{-\tau}\frac{1}{C^*C}\left(\rho A^* A^\mu + B^* B^\mu\right)\frac{dz}{z} \\
&\quad +\lambda_u \frac{1}{2\pi i}\oint z^{-\tau}\frac{C^\mu}{C^* C^2}\underbrace{\left(-\rho A^* A - B^* B\right)}_{-CC^*}\frac{dz}{z} \\
&= \lambda_u \frac{1}{2\pi i}\oint z^{-\tau}\frac{1}{C^*C}\left(-\rho A A^{*\mu} - B B^{*\mu} + C C^{*\mu}\right)\frac{dz}{z} \\
&= -\lambda_u \frac{1}{2\pi i}\oint z^{\tau}\frac{1}{C^*C}\left(\rho A^* A^\mu + B^* B^\mu - C^* C^\mu\right)\frac{dz}{z} \\
&= -\mathsf{E}\varepsilon(t-\tau,\boldsymbol{\theta}_0)\frac{\partial}{\partial\boldsymbol{\theta}_\mu}\varepsilon(t,\boldsymbol{\theta}_0)
\end{aligned} \tag{115}
$$

When considering (115) specifically for $\tau = 0$ one finds that

$$
\mathsf{E}\varepsilon(t,\boldsymbol{\theta}_0)\frac{\partial}{\partial\boldsymbol{\theta}_\mu}\varepsilon(t,\boldsymbol{\theta}_0) = 0 \tag{116}
$$

which is though something already known (as $\boldsymbol{\theta}_0$ is the minimizing point of $V_{31}(\boldsymbol{\theta})$), see (64).

Introduce also the square Sylvester matrix of dimension $n_a + n_b + 1$

$$
\mathbf{S} = \begin{pmatrix}
0 & b_0 & \dots & b_{n_b} & & \\
 & & \ddots & & \ddots & \\
 & & & b_0 & \dots & b_{n_b} \\
-1 & -a_1 & \dots & -a_{n_a} & & \\
 & \ddots & & & \ddots & \\
 & & -1 & & \dots & -a_{n_a}
\end{pmatrix}, \tag{117}
$$

and the matrices

$$
\mathbf{A}^\mu = \begin{pmatrix} \alpha^1 \\ \vdots \\ \alpha^{n_a+n_b+1} \end{pmatrix}, \quad \mathbf{B}^\mu = \begin{pmatrix} \beta^1 \\ \vdots \\ \beta^{n_a+n_b+1} \end{pmatrix}, \tag{118}
$$

where, with some abuse of notations, the row vectors consist of the individual polynomial coefficients. Then it holds

$$
\begin{aligned}
\mathsf{E}\psi(t)\psi^T(t) &= \mathbf{S}\ \mathrm{cov}\begin{pmatrix} \frac{1}{AC}u_0(t) \\ \vdots \\ \frac{1}{AC}u_0(t-n_a-n_b) \end{pmatrix}\mathbf{S}^T \\
&+\rho\lambda_u\mathbf{A}^{\mu}\mathrm{cov}\begin{pmatrix} \frac{1}{C^2}v(t) \\ \vdots \\ \frac{1}{C^2}v(t-n_a-n_b) \end{pmatrix}\mathbf{A}^{\mu T} \\
&+\lambda_u\mathbf{B}^{\mu}\mathrm{cov}\begin{pmatrix} \frac{1}{C^2}v(t) \\ \vdots \\ \frac{1}{C^2}v(t-n_a-n_b) \end{pmatrix}\mathbf{B}^{\mu T},
\end{aligned} \tag{119}
$$

where $v(t)$ denotes a white noise process of unit variance.

To find a way to compute the second term in (73), differentiating (113), evaluating it for $\boldsymbol{\theta} = \boldsymbol{\theta}_0$, and neglecting the part consisting of filtered $u_0(t)$ (recall that $\varepsilon(t, \boldsymbol{\theta}_0)$ is uncorrelated with any filtered version of $u_0(t)$) gives

$$
\begin{aligned}
& \frac{\partial^2}{\partial\boldsymbol{\theta}_\nu\partial\boldsymbol{\theta}_\mu}\varepsilon(t,\boldsymbol{\theta}) \\
= & -\frac{A^\mu C^\nu}{C^2}y(t) + \frac{B^\mu C^\nu}{C^2}u(t) - \frac{C^{\mu\nu}}{C^2}y(t)\left(Ay(t)-Bu(t)\right) \\
& +\frac{2C^\mu C^\nu}{C^3}\left(Ay(t)-Bu(t)\right) - \frac{C^\mu}{C^2}\left(A^\nu y(t) - B^\nu u(t)\right) \\
= & \left(-\frac{A^\mu C^\nu}{C^2} - \frac{A^\nu C^\mu}{C^2} - \frac{AC^{\mu\nu}}{C^2} + 2\frac{AC^\mu C^\nu}{C^3}\right)\tilde{y}(t) \\
& + \left(\frac{B^\mu C^\nu}{C^2} + \frac{B^\nu C^\mu}{C^2} + \frac{BC^{\mu\nu}}{C^2} - 2\frac{BC^\mu C^\nu}{C^3}\right)\tilde{u}(t) \\
\triangleq & \ \frac{\alpha^{\mu\nu}}{C^3}\,\tilde{y}(t) - \frac{\beta^{\mu\mu}}{C^3}\,\tilde{u}(t).
\end{aligned} \tag{120}
$$

It is clear that the expression in (120) can be interpreted as the sum of two independent ARMA processes, driven by the white noise processes $\tilde{y}(t)$ and $\tilde{u}(t)$, respectively. To compute the second term in (73) is then a standard problem for computing cross-covariances.

The term $\mathsf{E}\varepsilon(t)\varepsilon^{''}(t)$ is evaluated component-wise as

$$
\begin{aligned}
\mathsf{E}\varepsilon(t)\varepsilon^{''}(t)_{\mu\nu} &= \rho\ \lambda_u\mathsf{E}\left\{\frac{A}{C}v(t)\frac{\alpha^{\mu\nu}}{C^3}v(t)\right\} \\
&+\lambda_u\mathsf{E}\left\{\frac{B}{C}v(t)\frac{\beta^{\mu\nu}}{C^3}v(t)\right\},
\end{aligned} \tag{121}
$$

where again $v(t)$ is a white noise process of unit variance.

Next consider the sum in (74). As $\varepsilon(t)$ is uncorrelated of $u_0(s)$ for all t and s, it holds

$$\begin{aligned} \mathsf{E}\left\{\varepsilon(t+\tau)\psi_\mu(t)\right\} &= \mathsf{E}\left\{\frac{A}{C}\tilde{y}(t+\tau)\frac{\alpha^\mu}{C^2}\,\tilde{y}(t)\right\} \\ &\quad +\mathsf{E}\left\{\frac{B}{C}\tilde{u}(t+\tau)\frac{\beta^\mu}{C^2}\,\tilde{u}(t)\right\} \end{aligned} \tag{122}$$

The following lemma can be conveniently applied for the evaluation of an infinite sum of cross-covariances. The lemma is proved in Söderström and Mossberg (2011).

Lemma D.1 *Consider the ARMA processes*

$$\begin{aligned} x_1(t) &= \frac{B_1(q^{-1})}{A_1(q^{-1})}e(t) \qquad x_2(t) = \frac{B_2(q^{-1})}{A_2(q^{-1})}e(t), \\ x_3(t) &= \frac{C_1(q^{-1})}{D_1(q^{-1})}v(t) \qquad x_4(t) = \frac{C_2(q^{-1})}{D_2(q^{-1})}v(t), \end{aligned} \tag{123}$$

where $e(t)$ and $v(t)$ are zero mean white noise sequences, possibly correlated, and of unit variances. Then it holds that

$$\begin{aligned} \sum_{\tau=-\infty}^{\infty} r_{x_1x_2}(\tau)r_{x_3x_4}(\tau) &= \mathsf{E}\left[\frac{B_2(q^{-1})}{A_2(q^{-1})}\frac{C_1(q^{-1})}{D_1(q^{-1})}e_0(t)\right] \\ &\quad \times\left[\frac{B_1(q^{-1})}{A_1(q^{-1})}\frac{C_2(q^{-1})}{D_2(q^{-1})}e_0(t)\right], \end{aligned} \tag{124}$$

where $e_0(t)$ is white noise with unit variance.

This trick can be applied to compute the different matrix elements of the sum in (74).

Using Lemma D.1 leads to

$$\begin{aligned} & \left[\sum_{\tau=-\infty}^{\infty}\left(\mathsf{E}\varepsilon(t+\tau)\psi(t)\right)\left(\mathsf{E}\varepsilon(t-\tau)\psi(t)\right)\right]_{\mu\nu} \\ = & \sum_{\tau=-\infty}^{\infty} r_{\varepsilon\psi_\mu}(\tau)r_{\varepsilon\psi_\nu}(-\tau) \\ = & \ \rho^2\lambda_u^2\mathsf{E}\left\{\frac{\alpha^\mu\alpha^\nu}{C^4}v(t)\frac{A^2}{C^2}\,v(t)\right\} \\ & +\lambda_u^2\mathsf{E}\left\{\frac{\beta^\mu\beta^\nu}{C^4}v(t)\frac{B^2}{C^2}\,v(t)\right\} \\ & +\rho\lambda_u^2\mathsf{E}\left\{\frac{\alpha^\mu\beta^\nu}{C^4}v(t)\frac{AB}{C^2}\,v(t)\right\} \\ & +\rho\lambda_u^2\mathsf{E}\left\{\frac{\alpha^\nu\beta^\mu}{C^4}v(t)\frac{AB}{C^2}\,v(t)\right\}, \end{aligned} \tag{125}$$

with $v(t)$ being a white noise of unit variance.

References

Agüero, J. C., J. I. Yuz, G. C. Goodwin and R. A. Delgado (2010). 'On the equivalence of time and frequency domain maximum likelihood estimation'. *Automatica* **46**(2), 260–270.

Cadzow, J. A. and O. M. Solomon (1986). 'Algebraic approach to system identification'. *IEEE Transactions on Acoustics, Speech and Signal Processing* **ASSP-34**(3), 462–469.

Diversi, R., R. Guidorzi and U. Soverini (2007). 'Maximum likelihood identification of noisy input-output models'. *Automatica* **43**, 464–472.

Fernando, K. V. and H. Nicholson (1985). 'Identification of linear systems with input and output noise: the Koopmans–Levin method'. *IEE Proceedings, Part D* **132**(1), 30–36.

Guidorzi, R., R. Diversi and U. Soverini (2008). 'The Frisch scheme in algebraic and dynamic identification problems'. *Kybernetika* **44**(5), 585–616.

Lindley, D. V. (1947). 'Regression lines and the linear functional relationship'. *Supplement to the Journal of the Royal Statistical Society* **9**(2), 218–244.

Ljung, L. (1999). *System Identification - Theory for the User, 2nd edition*. Prentice Hall. Upper Saddle River, NJ, USA.

McKelvey, T. (2002). 'Frequency domain identification methods'. *Circuits, Systems and Signal Processing* **21**(1), 39–55.

Pintelon, R. and J. Schoukens (2007). 'Frequency domain maximum likelihood estimation of linear dynamic errors-in-variables models'. *Automatica* **43**(4), 621–630.

Pintelon, R. and J. Schoukens (2012). *System Identification. A Frequency Domain Approach, 2nd edition*. Wiley. Hoboken, NJ, USA.

Pintelon, R., J. Schoukens and G. Vandersteen (1997). 'Frequency domain system identification using arbitrary signals'. *IEEE Transactions on Automatic Control* **42**(12), 1717–1720.

Schoukens, J., R. Pintelon, G. Vandersteen and P. Guillaume (1997). 'Frequency domain system identification using non-parametric noise models estimated from a small number of data sets'. *Automatica* **33**, 1073–1086.

Söderström, T. (1981). 'Identification of stochastic linear systems in presence of input noise'. *Automatica* **17**, 713–725.

Söderström, T. (2002). *Discrete-time Stochastic Systems - Estimation and Control, 2nd edition*. Springer-Verlag. London, UK.

Söderström, T. (2007). ‘Errors-in-variables methods in system identification’. *Automatica* **43**(6), 939–958. Survey paper.

Söderström, T. (2011). ‘A generalized instrumental variable estimation method for errors-in-variables identification problems’. *Automatica* **47**(8), 1656–1666.

Söderström, T. (2012). ‘System identification for the errors-in-variables problem’. *Transactions of the Institute of Measurement and Control* **34**(7), 780–792.

Söderström, T. and M. Mossberg (2011). ‘Accuracy analysis of a covariance matching approach for identifying errors-in-variables systems’. *Automatica* **47**(2), 272–282.

Söderström, T. and P. Stoica (1989). *System Identification*. Prentice Hall International. Hemel Hempstead, UK.

Söderström, T., M. Mossberg and M. Hong (2009). ‘A covariance matching approach for identifying errors-in-variables systems’. *Automatica* **45**(9), 2018–2031.

Söderström, T., U. Soverini and K. Mahata (2002). ‘Perspectives on errors-in-variables estimation for dynamic systems’. *Signal Processing* **82**(8), 1139–1154.

Soverini, U. and T. Söderström (2014). Frequency domain maximum likelihood identification of noisy input-output models. In ‘Proc. 19th IFAC World Congress’. Cape Town, South Africa.

Van Huffel, S. and Lemmerling, P. (Eds.) (2002). *Total Least Squares and Errors-in-Variables Modelling. Analysis, Algorithms and Applications*. Kluwer. Dordrecht, The Netherlands.

Van Huffel, S. (Ed.) (1997). *Recent Advances in Total Least Squares Techniques and Errors-in-Variables Modelling*. SIAM. Philadelphia, USA.

Zhang, E., R. Pintelon and J. Schoukens (2013). ‘Errors-in-variables identification of dynamic systems excited by arbitrary non-white input’. *Automatica* **49**(12), 3032–3041.